Scanning Microscopy

Volume 9 | Number 1 Article 6

3-5-1995

Etiology of Calcium Oxalate Nephrolithiasis in Rats. I. Can This Be a Model for Human Stone Formation?

W. C. de Bruijn
Erasmus University Rotterdam, de_bruijn@pa1.fgg.eur.nl

E. R. Boevé
Academic Hospital Rotterdam

P. R. W. A. van Run
Erasmus University Rotterdam

P. P. M. C. van Miert
Academic Hospital Rotterdam

R. de Water
Academic Hospital Rotterdam

See next page for additional authors

Etiology of Calcium Oxalate Nephrolithiasis in Rats. I. Can This Be a Model for Human Stone Formation?

Authors

W. C. de Bruijn, E. R. Boevé, P. R. W. A. van Run, P. P. M. C. van Miert, R. de Water, J. C. Romijn, C. F. Verkoelen, L. C. Cao, and F. H. Schröder

Scanning Microscopy, Vol. 9, No. 1, 1995 (Pages 103-114) 0891-7035/95$5.00+.25
Scanning Microscopy International, Chicago (AMF O'Hare), IL 60666 USA

ETIOLOGY OF CALCIUM OXALATE NEPHROLITHIASIS IN RATS. I. CAN THIS BE A MODEL FOR HUMAN STONE FORMATION?

W.C. de Bruijn*, E.R. Boevé[1], P.R.W.A. van Run, P.P.M.C. van Miert[1], R. de Water[1], J.C. Romijn[1], C.F. Verkoelen[1], L.C. Cao[1] and F.H. Schröder[1]

AEM-unit, Clin. Pathology Inst., Erasmus Univ. Rotterdam, [1]Dept. Urology, Academic Hospital Rotterdam, P.O. Box 1738, 3000 DR Rotterdam, The Netherlands

(Received for publication December 5, 1994 and in revised form March 5, 1995)

Abstract

Crystal retention is studied in a rat-model system as a possible mechanism for the etiology of human nephrolithiasis. A crystal-inducing diet (CID) of ethylene glycol plus NH_4Cl in their drinking-water is offered to healthy rats to generate intratubular crystals. Subsequently, the fate of retained crystals is investigated by allowing the rats a tissue recovery/crystalluria phase for three, five and ten days, respectively, on normal drinking water.

The process of exotubulosis is observed in cortex and medulla of aldehyde-fixed kidneys after three days recovery. After five days, crystals are predominantly seen there in the interstitium. After ten days, cortex and medulla are virtually free of crystals. However, in the papillary regions after five and ten days recovery, three types of calcium oxalate monohydrate (COM) crystals are present: (1) free in the calycine space, (2) sub-epithelially located surrounded by interstitial cells within, and (3) covered by macrophage-like cells, outside the original papillary surface. After a CID plus three days recovery, a further thirty-seven days extra oxalate challenge with solely 0.3 vol% ethylene glycol induced intratubular and interstitial oxalate crystals. In the papillary region, large sub-epithelial crystals are seen. However, no crystals are seen in kidneys from rats given solely (0.5 or 0.8 vol. %) ethylene glycol for thirty days. An oxalate re-challenge retards crystal removal.

Key Words: Calcium oxalate, urolithiasis, rat model, transmission electron microscopy, papillary lesions.

*Address for correspondence:
W.C. de Bruijn,
AEM-unit, Clinical Pathology Institute, Ee902,
Erasmus University Rotterdam, FGG.
P.O. Box 1738,
3000 DR Rotterdam, The Netherlands.
Telephone number: 31-10-4087922
FAX number: 31-10-436 6660
E.Mail: de Bruijn@PA1.FGG.EUR.nl

Introduction

Investigations on etiology of human nephrolithiasis are hampered by the fact that only relatively final stone-disease development stages can be studied. Deductive studies previously performed on autopsy series [30] or analysis of collected stones [5, 6, 14, 28, 29] have induced concepts about human nephrolithiasis [30], which may be improved in the light of recent observations. Animal model systems are a prerequisite for inductive investigations about the early events, although they involve the risk of studying possibly totally different mechanisms of stone formation. Healthy rats have frequently been used to induce calcium oxalate mono- or di-hydrate (COM and/ or COD) crystalluria and/or crystal retention to mimic the etiology of that type of human stone formation [1-3, 8-12, 15-16, 20, 22-24, 34-36]. The presence of crystals in the intratubular space along the nephron has been considered to play an important role in the etiology of nephrolithiasis. Crystal growth and/or agglomeration, promoted or inhibited there by endogenous and/or exogenous chemical compounds [3, 13, 17, 26-27, 31-33], are considered the main driving force for nephrolithiasis or its prevention [4].

Intratubular crystals can be induced within minutes by intraperitoneal (i.p.) or intravenous (i.v.) injections with oxalate salts [18, 21, 22]. Crystal induction is related to cellular injury [12, 21]. A more chronic situation can be created through a crystal inducing diet (CID) over seven to thirty days. In that case, the animal's drinking water is supplemented with ethylene glycol (EG), which is converted to oxalic acid in the liver, completed with additions of either ammonium chloride (AC) or vitamin D_3 [2, 6, 8, 9].

Previously, we have shown the presence of calcium contents and crystalline character in intracellularly retained COM crystals in proximal and distal tubule cells, in addition to intratubular crystals, after an eight days CID with EG plus AC [2, 8]. Recently, we have described an additional process of crystal retention and the fate of such retained intratubular crystals in the cortical and medullar region using this rat-model system with a

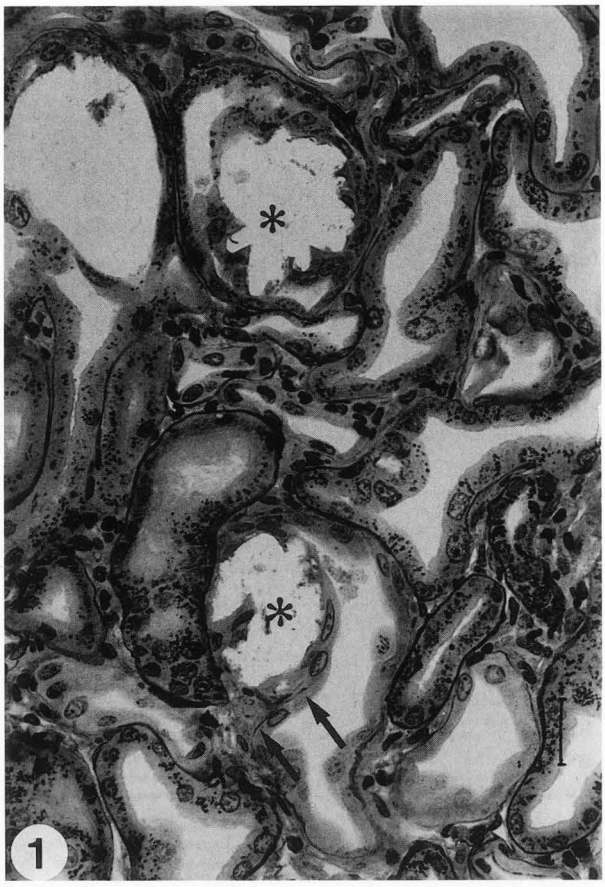

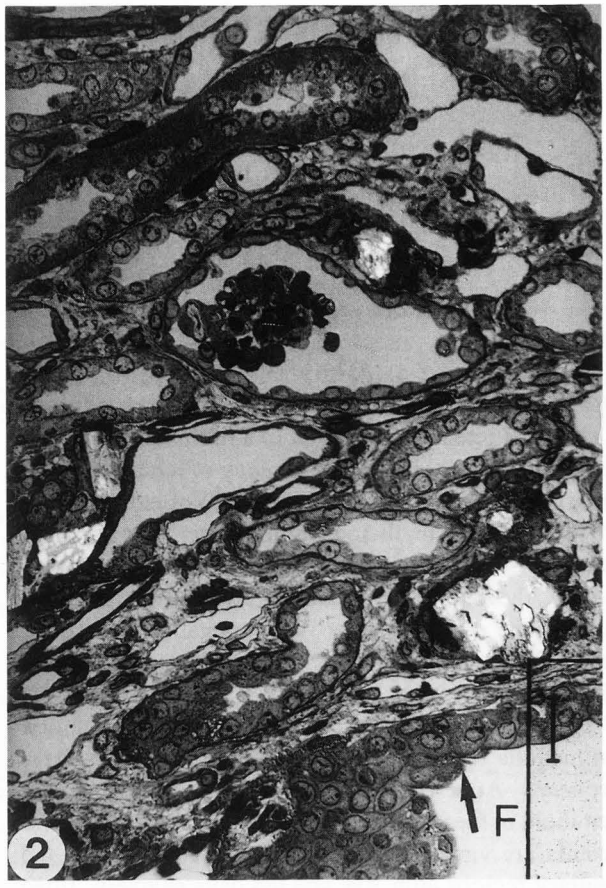

Figures 1-10. Light micrographs of rat kidney after CID plus three (Figs. 1 and 2), five (Figs. 3 to 6) and ten (Figs. 7-10) days recovery periods. Figure 1. Exotubulosis with ghosts of crystal agglomerates (*), arrows point to new basement membrane material (↓). The crystal bi-refringence is lost. GMA, Jones, Crossed Nicol prisms. Bar = 25 μm. **Figure 2.** Exotubulosis in the papillary area with crystal agglomerates (*). F = fornix with cuboidal cells (↑) covering the original papillary surface. Epon, Toluidine blue, Crossed Nicol prisms. Bar = 25 μm.

---

similar nine-days CID [9]. We have shown that in CID rats, after a two days post-induction recovery/crystalluria phase on normal drinking water, not all intratubular crystals have disappeared. Crystals retained at the apex of cortical and medullar tubular lining cells are subsequently overgrown by neighbouring epithelial cells. These epithelial cells form basement membrane material at their basal side, isolating the crystalline material from the tubular lumen, and in that way, relocating the crystals in the interstitium; a process which has been proposed to be called: exotubulosis. After an additional regime of twelve and forty-two days on solely 0.1 vol.% EG, assumed to create a low-oxalate challenge, no intratubular crystals have been observed; however, free interstitial crystal agglomerates and cell-bound crystals, some in Giant cells, have been seen, resembling certain forms of human nephrolithiasis [19].

In the present study, a nine days CID is used to further investigate:

(1) the fate of the induced crystal mass without a subsequent oxalate challenge;

(2) the fate of the induced crystal mass after a subsequent more pronounced oxalate challenge, to allow crystals to be eventually converted into mini-stones; and

(3) whether papillary parts of the nephron and the calycine space are affected.

A regime to obtain these objectives includes the following additional treatments:

(a) increasing the post-induction recovery phase to three, five and ten days;

(b) increasing the EG concentration after a three days post-induction recovery phase from 0.1 vol.% as given before [9] to 0.3 vol.% to assure a sufficiently high renal oxalate level during the subsequent thirty-seven days period; and

(c) giving the animals solely EG (0.5 or 0.8 vol% without AC) for thirty days.

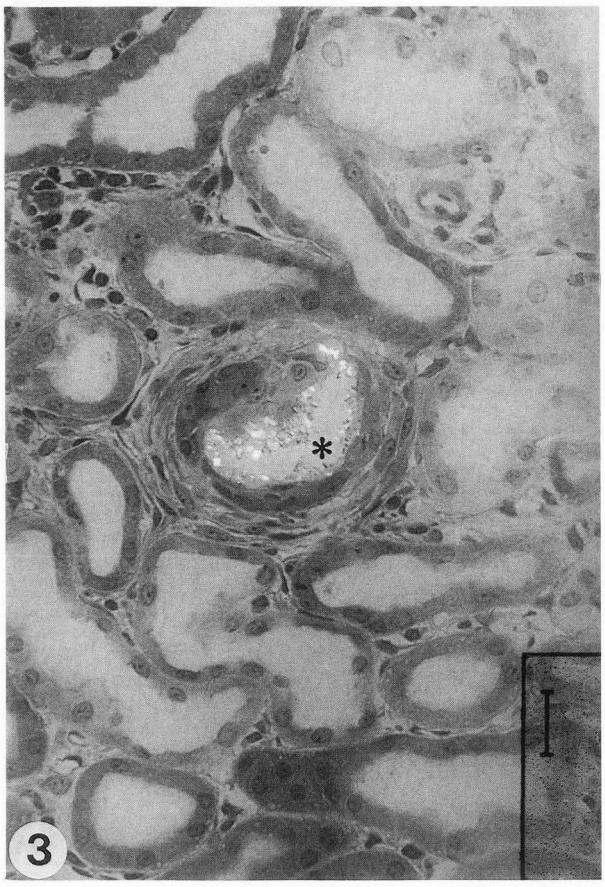

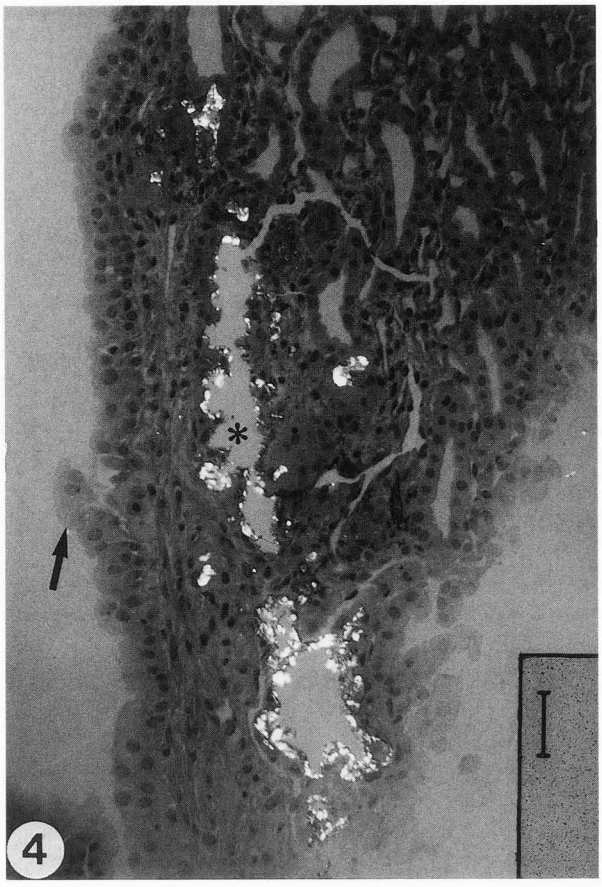

Figure 3. Interstitial crystal agglomerate in the cortex (*). GMA, Haematoxylin/Azophloxine, Crossed Nicol prisms. Bar = 25 μm. **Figure 4**. Crystal masses beneath the papillary surface (*), cuboidal cells (↓) covering the original papillary surface. GMA, Haematoxylin/Azophloxine, Crossed Nicol prisms. Bar = 50 μm.

Attention will be concentrated on the papillary changes and on the papillary surface.

Material and Methods

Male Wistar rats (weighing about 250 g) from the Erasmus Animal Science Centre were acclimatized and kept on a normal rat chow. At the start of the experiment, their drinking water was supplemented with 0.8 vol. % ethylene glycol plus 1 wt. % NH_4Cl for nine days. To confirm the presence of intratubular crystals, rats were sacrificed directly after this nine-days CID period [2].

After this nine-days CID period, all rats were kept on normal drinking water without additions for three, five and ten days, respectively. During this post-induction phase, it was assumed that all non-retainable intratubular crystals were removed by crystalluria. In the mean time, this regime may have introduced a recovery in the tissue from the acute effects of the CID. This post-induction crystalluria/recovery regime will be called recovery phase in the remainder of this paper.

Other rats were, after a three days post-induction recovery phase, re-challenged with oxalate, by re-supplementing the drinking water with (0.1 or) 0.3 vol. % EG without NH_4Cl for thirty-seven days duration. Again, three days of normal drinking water was included in the regime at the end of that challenge [9].

In control rats, kept on a drinking regime of 0.5 vol. % or 0.8 vol. % EG without NH_4Cl for thirty days, the crystal inducing capacity of that regime was verified. At the end, three days of normal drinking water was included.

All rat kidneys were fixed by vascular perfusion with glutaraldehyde in cacodylate/HCl buffer as described before [2]. All removed kidneys were examined by X-ray *in toto* for possible crystal/stone locations.

One to two mm-thick slices were ethanol dehydrated and embedded in glycol methacrylate (GMA). Three to four μm-thick GMA sections were examined under crossed Nicol prisms for crystal locations. Section stains included haematoxylin/azophloxine and two

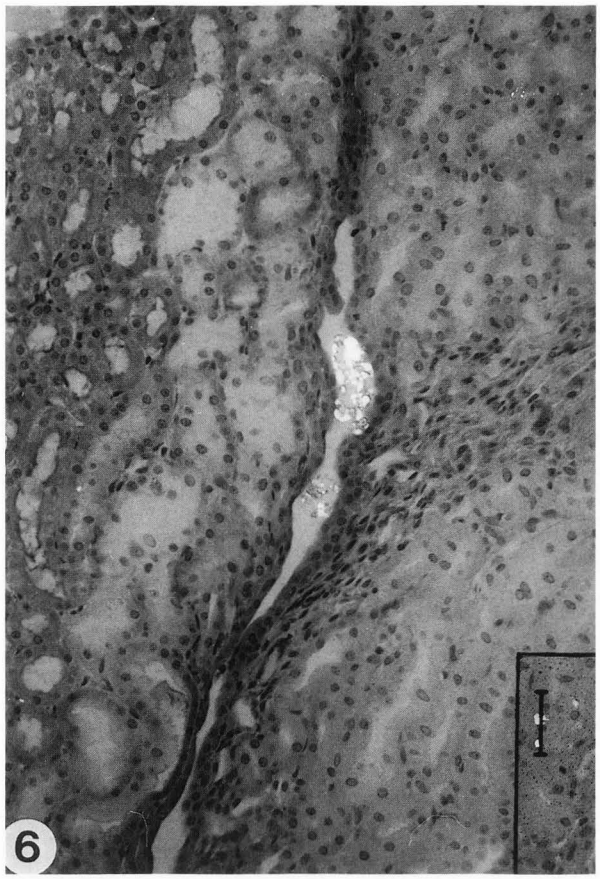

Figure 5. Crystal masses at the papillary surface covered by cuboidal cells and free in the calycine space (*). GMA, Haematoxylin/Azophloxine, Crossed Nicol prisms. Bar = 25 μm. **Figure 6**. Crystal masses free in the calycine space not covered by cells (*). GMA, Haematoxylin/Azophloxine, Crossed Nicol prisms. Bar = 50 μm.

basement membranes stains: viz., periodic acid Schiff and Jones. In addition, a calcium localizing Von Kossa staining was used.

For ultrastructural observations, millimeter-thick slices were postfixed by osmium tetroxide plus ferrocyanide and epon embedded, as described before [7]. Unstained, or uranyl acetate/lead citrate stained ultrathin epon sections on 400 mesh grids without films or parlodion filmed grids were examined in a Zeiss EM902 transmission electron microscope (Zeiss, Oberkochen, Germany) and micrographs were recorded in an analogue way on sheet film.

Results

Light microscopy (LM)

The cortex and medulla of rats with a three days post-induction recovery phase showed luminal crystal retention and signs of exotubulosis (Fig. 1), similar as described before [9]. In the inner band of the outer zone of the papilla, a similar intratubular crystal distribution and aspects of exotubulosis were observed (Fig. 2). The presence of interstitial crystals was confirmed by application of Von Kossa's stain, which converts the bi-refringent material into black precipitates, leaving the remainder of the peri-tubular spaces unstained (see below). Large interstitial crystal-containing spaces below the papillary surface were seen. Desquamation of the cells from ducts of Bellini was infrequently observed (not shown).

In CID rats after five days recovery, predominantly interstitial crystal localizations were seen both in cortex and medulla (Fig. 3). In the inner band of the outer zone of the papilla, crystals were seen: as large interstitial spaces below the papillary surface (Fig. 4), at the papillary surface but surrounded by a thin layer of cells, forming a pseudo-stratified epithelial layer (Fig. 5) and free in the calycine space (Figs. 5 and 6). A pseudo-urothelium covered the original papillary surface (Figs. 2, 4, and 5). Incidently, crystals were seen in the wall of the calyx towards the ureter (not shown).

After a ten days post-induction recovery phase, interstitial crystals were rarely seen in the cortical or

Figure 7. Interstitial crystal agglomerate in the papilla (*) at the fornix. GMA, Haematoxylin/Azophloxine, Crossed Nicol prisms. Bar = 50 μm. **Figure 8**. Crystal agglomerate in the fornix (*), with cells in the immediate surroundings. GMA, Haematoxylin/ Azophloxine, Crossed Nicol prisms. Bar = 25 μm.

---

medullar region (not shown). At the papillary zone, interstitial crystal masses (Fig. 7) and free crystals located in the calycine space (Fig. 8) were seen. Large crystalline masses were seen in a sub-epithelial zone (Fig. 9). The Von Kossa staining converts the bi-refringent interstitial crystalline material into black precipitates (Fig. 10).

After the additional oxalate challenge with 0.3% EG for thirty-seven days, large interstitial crystal agglomerates were seen in both the cortical (Fig. 11) and medullar region, surrounded by inflammatory cells. In the papilla, interstitial crystals (Fig. 12), as well as subepithelial crystal masses without a sign of inflammation (not shown), were seen. No crystals were seen in the kidneys from rats challenged only with either 0.5 or 0.8% EG without any additives for thirty days (not shown).

Transmission electron microscopy (TEM)

Figure 13, relates LM to TEM image details from exotubulosis in the papillary region, after a three days post-induction recovery phase. The inset of Figure 13 shows final stages in the exotubulosis process in this papillar region (↓). In the TEM image, the original lumen (*) as well as a large crystalline mass (♦) can be recognized. Epithelial cells were present at the luminal side of the (newly synthesized?) tubular basement membrane. The crystalline mass below the basement membrane was partially surrounded by interstitial cells. Arrowheads (▲) point to artifacts giving false-positive crystal-localizations due to crystal displacement during sectioning.

From the same kidney, Figures 14, 15 and 16 show a dome-shaped crystal mass bulging into the calycine space. The LM inset in Figure 14 shows the entire area. A layer of cuboidal cells is present on top of the original papillary surface. The squares indicate the position of Figures 14, 15 and 16. Details at the luminal apex (Fig. 14) show crystal ghosts surrounded by monocytic cells embedded in a fibrous interstitial matrix. Some cells show crystal internalization (↑). The cells covering the crystal mass have a pseudo-stratified epithelial architecture, and rounded forms with rather flat

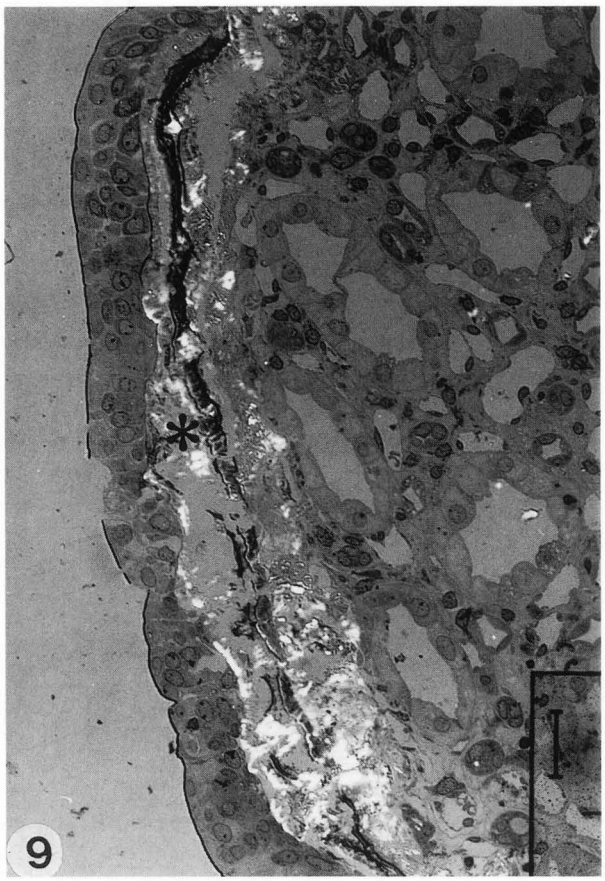

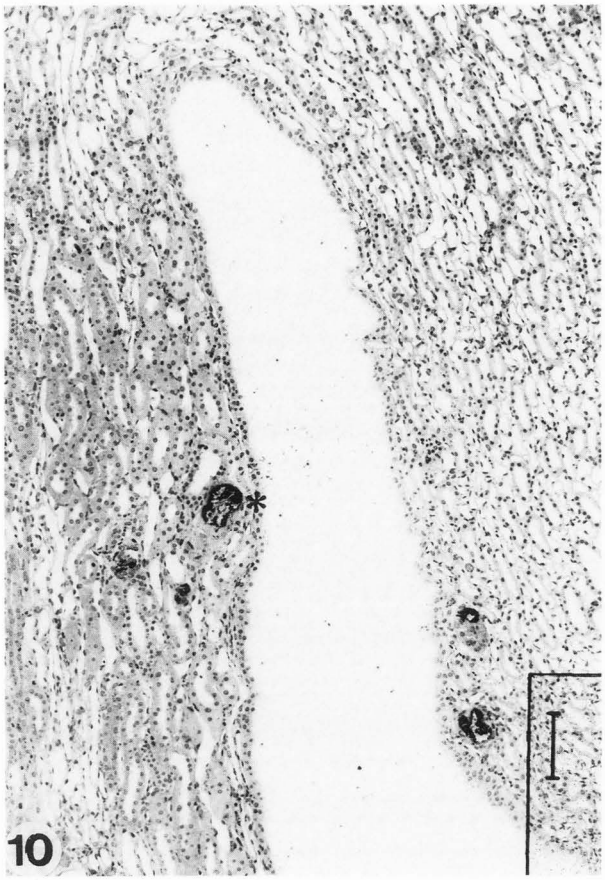

Figure 9. Crystal agglomerate in the interstitium of a cross-sectioned papillary region (*), covered by a pseudo-stratified layer of cuboidal cells. Epon, Toluidine Blue, Crossed Nicol prisms. Bar = 25 μm. **Figure 10**. Black precipitates in the crystal agglomerates (*) in the interstitium of a papillary region around the fornix. GMA, Von Kossa. Bar = 100 μm.

pseudopodia facing a basement membrane, and widened intercellular spaces. In some cells, lysosomes were seen. Figure 15 shows details of a basal portion of the centrally located crystal mass. In the crystal ghosts present, growth rings are visible (↓), which are rather clear in the central portion of the crystal mass outside this area (not shown). Details from the site of the dome (Fig. 16) show that the covering cell layer is extremely thin. In the interstitial fibrous matrix, some small crystal ghost are reaching out just beneath this cell layer. The bulk of the crystal ghosts at the left, with a typical complex morphology, is surrounded by cell debris.

An ultrathin section from crystalline material at the basis of such a sub-epithelial mass, shown in Figure 17, indicates that the interstitial crystals have no relation with any peri-tubular pre-calculus material. The inset compares the acquired electron diffraction pattern from crystals at this site to those from pure COM crystals.

The kidney morphology after five and ten days post-induction recovery phase are shown in detail in an accompanying paper relating scanning electron microscopy (SEM) and LM observations from the same papilla [10].

Discussion

The present investigation shows:

(1) that exotubulosis, shown before [9] in the cortical and medullar zones, is also present in the papillary region; hence, exotubulosis occurs along the whole nephron following crystal retention at the apex of tubular-lining cells.

(2) the fate of interstitial crystals removed by exotubulosis: a ten days post-induction recovery phase leads to crystal removal from the cortical/medullary zones.

(3) the presence of interstitial crystal masses in the papillary zones at peripheral places protruding into the calycine space. In the case of a three days recovery phase, the surface covering the crystal mass is irregular, but not broken. In the case of five or ten days recovery,

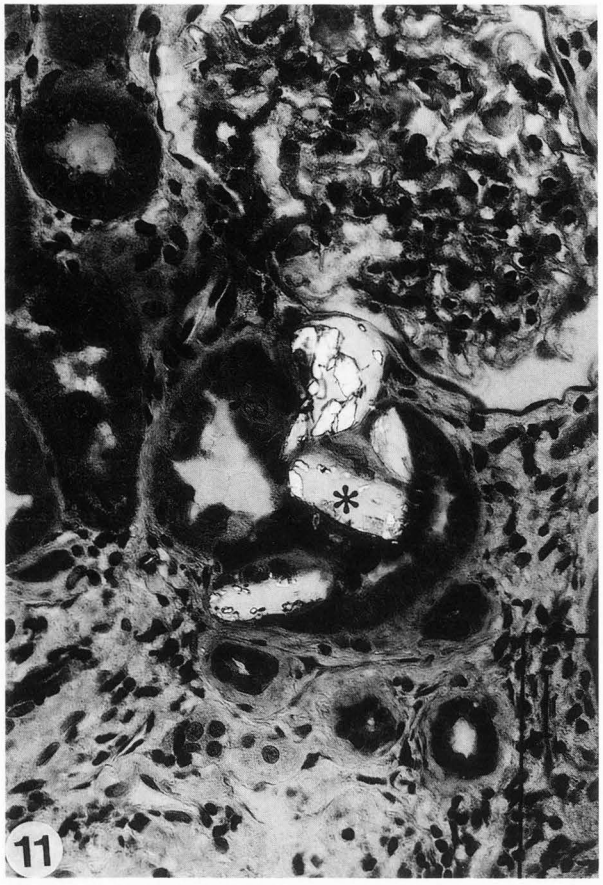

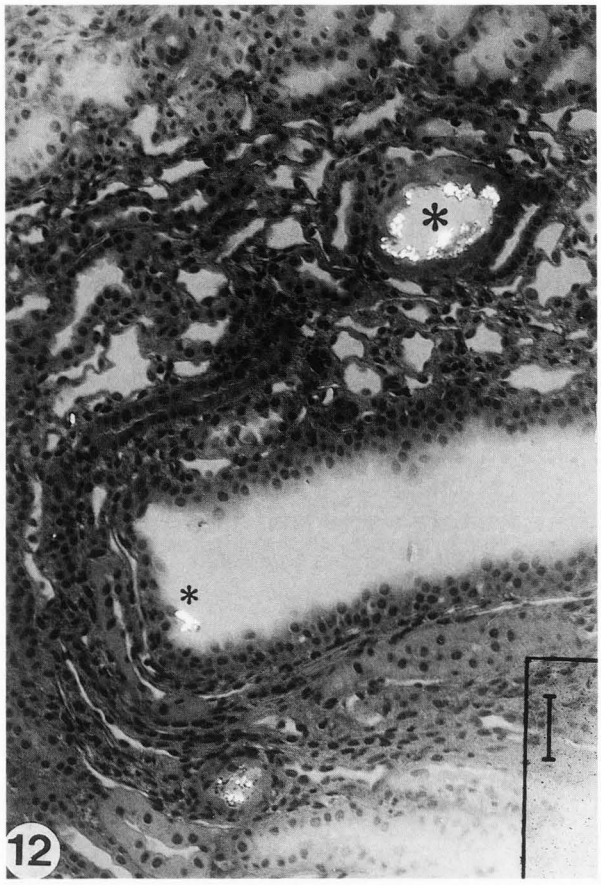

Figures 11-12. Light micrographs of rat kidney after CID plus three days recovery, plus a thirty-seven days 0.3 vol% EG regime. Crystal masses in the cortical interstitium surrounded by inflammatory cells (**Figure 11**); and in an interstitial papillary cleft (**Figure 12**), a layer of cuboidal cells covers the papillary surface. GMA, Haematoxylin/Azophloxine, Crossed Nicol prisms. Bars = 50 μm (Fig. 11) and 100 μm (Fig. 12).

---

free crystals are seen in the calycine space, attached to the surface or surrounded by cuboidal cells, creating a pseudo-stratified epithelial cover around them. Also, large sub-epithelial interstitial crystal masses are present.

(**4**) that interstitial crystals are still present after a thirty-seven days additional regime with 0.3 vol% EG. This additional oxalate challenge maintains the presence of these crystals, retards their removal or stimulates their growth.

(**5**) that thirty days lasting regimes with only EG do not generate retained crystals in our rats.

The rat CID model presented shows aspects about the etiology of the crystal/cell interaction at places along the nephron and at the papillary surface. These observations might contain information about identical processes in human nephrolithiasis.

The intratubular presence of crystals after their acute induction (by i.p. or i.v. injections) and their fate and disappearance through crystalluria, has been shown before [18, 21, 22]. Khan *et al.* [22] have described the sequence of events leading to crystal formation on rat's papillary tips after a single i.p. dose of sodium oxalate of 7 mg/100 g body weight over a time span up to 336 hours after injection. Moreover, in the papillary tip, TEM showed crystals in a period between 6-24 hours in the ductal lumina, in the intercellular spaces, and in between or at the basal lamina in ducts of Bellini. The damage to the urothelial cells covering the crystals has been shown by both SEM and TEM observations, but complete recovery is seen after more than 72 hours. This acute episode might have been passed after our three days crystalluria/recovery phase. Similar observation have been obtained by Dijkstra and Hackett [11]. These changes have been related to cell injury and enzyme losses by Hackett *et al.* [15] and Khan *et al.* [22].

Aspects of crystal retention both in time and in place, plus the process of exotubulosis under more chronic conditions after nine days CID have been shown recently by us [8]. It is concluded now that exotubulosis apparently can be performed by all epithelial cells along

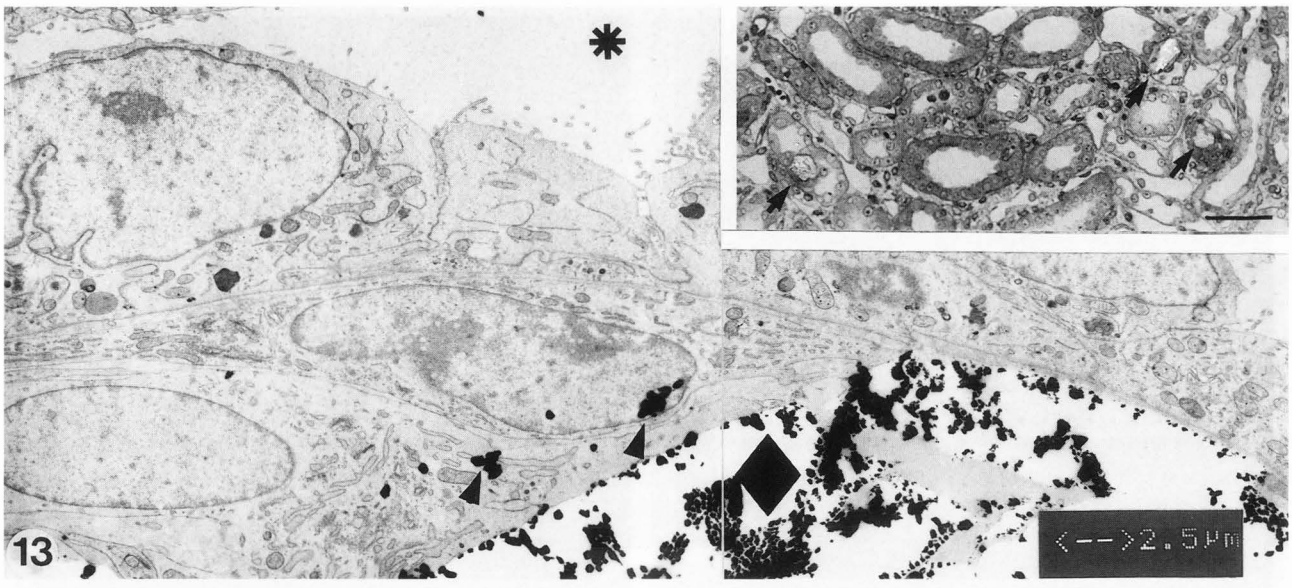

Figure 13 (above). Transmission electron micrograph showing exotubulosis in a papillary region. Tubular lumen (*); complex interstitial crystalline mass (♦). Arrowheads (▲) point to artifacts. Unstained section. **Inset.** Light micrograph showing stages of exotubulosis in the papillary region (↑). Bar = 7.5 µm.

Figures 14-16 (on the facing page). Micrographs of rat kidney after a three days post-induction recovery phase. **Figure 14 inset.** An area of crystals bulging into the calycine space. Squares indicate the position of Figures 14 to 16. Bar = 7.5 µm. **Figure 14-16.** Transmission electron micrographs at identical magnifications; uranyl acetate/lead citrate. **Figure 14** shows crystal ghosts (*) in the interstitial space surrounded by monocytes and covered by a layer of unidentified cells. Interstitial macrophages, show crystal endocytosis (↑). **Figure 15** shows crystal ghost at the base of the structure. In the ghost, growth rings are visible (↓). **Figure 16** shows crystal ghost in the interstitial space surrounded by cell debris and collagen fibrils and below a layer of unidentified cells.

---

the nephron, although a more precise recognition of the cell types involved is absent. This will be addressed in future experiments. The sequence of events in this chronic CID model [2], starts after about four days of the EG-drinking regime. The correlation between the tissue response and the amount of oxalate involved is lost. The effect of oxalate is determined by the rat's variability, their drinking habits, their conversion rate of ethylene glycol to oxalate in their liver, their oxalate excretion and their balance between crystal growth/aggregation stimulation and prevention. This leads to differences (as compared to the acute experiments) in the kidney with respect to the inorganic processes such as super- saturation, crystal formation, crystal sizes, and their coating by (glyco)proteinaceous substances. This needs further investigation.

Because ten days recovery removes virtually all cortical/medullary crystals, the present observations with an additional oxalate challenge by 0.3 vol% EG for thirty-seven days, confirm our previous observations [9]. It shows, as assumed previously [9], that the retained interstitial crystals, present in the rats submitted to an additional 0.1 vol% EG post-induction regime to generate a prolonged low-oxalate pressure in the kidneys, indeed did react accordingly in that forty-five days regime, although the magnitude of these oxalate challenges still are to be determined. Because it is established now that the fixed-particle retention process which can take place at any side along the nephron is an independent process that exists in addition to the free-particle retention process, the retention in the renal papilla as described by Grasses *et al.* [14], does not form an exceptional case. However, the concept of crystal growth proposed by them might have to be reconsidered now.

The presence of intra-tubular papillary calculi in collecting ducts, created in rats as described by Wright and Hodgkinson [36] by a high phosphorus-low vitamin B_6 diet and considered to start at the tubular basement membranes, is not confirmed by our observations. Desquamation of papillary collecting duct cells is not frequently observed in our rats, but this might have been restored during the recovery phase.

The structural description of the sub-epithelial calcium deposits at the LM level is, at first sight, similar to

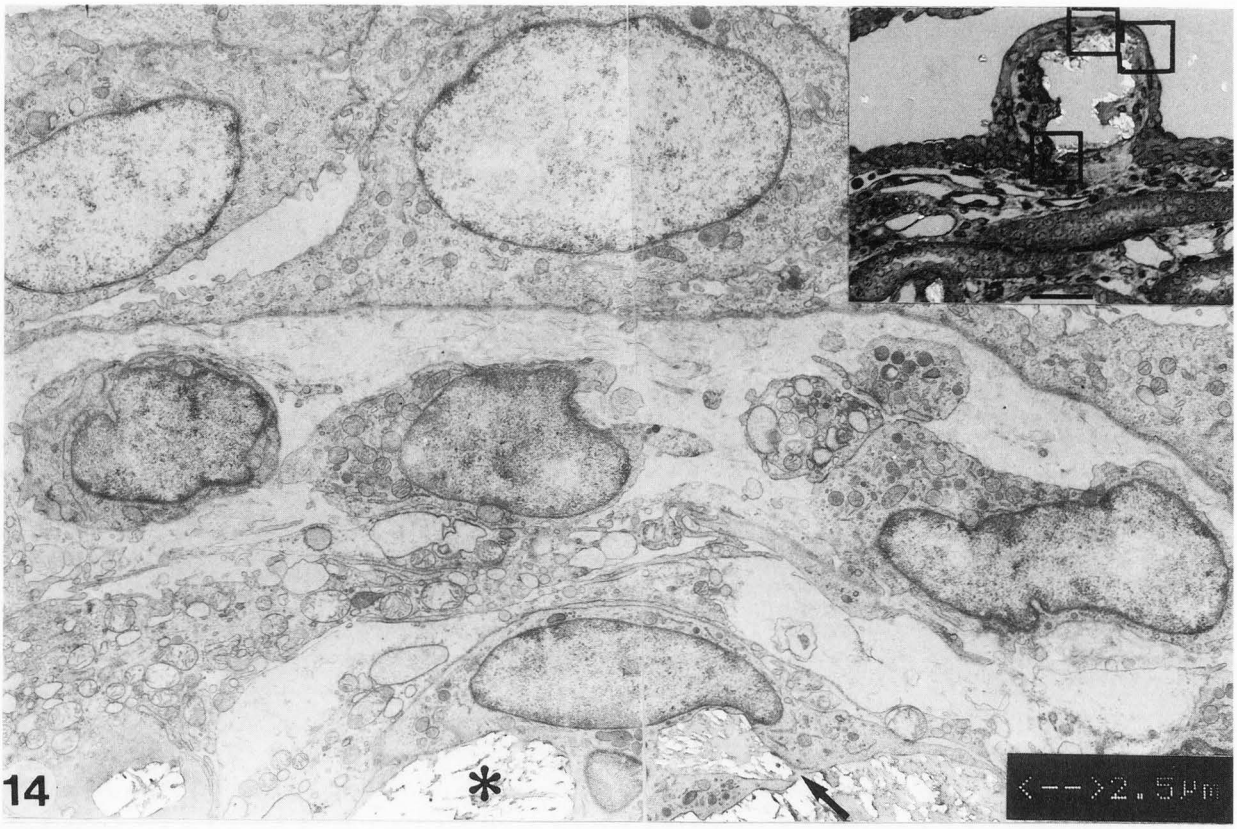
14
<--->2.5µm

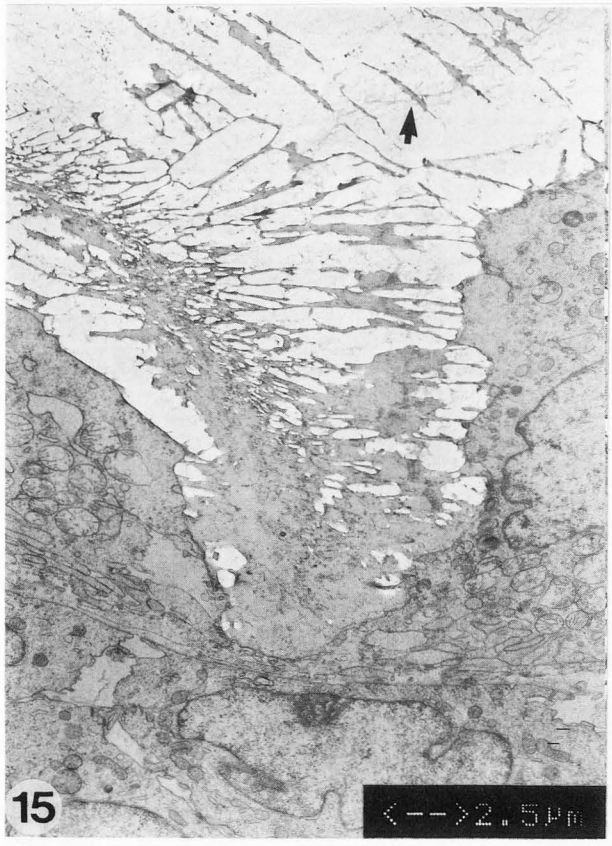
15
<--->2.5µm

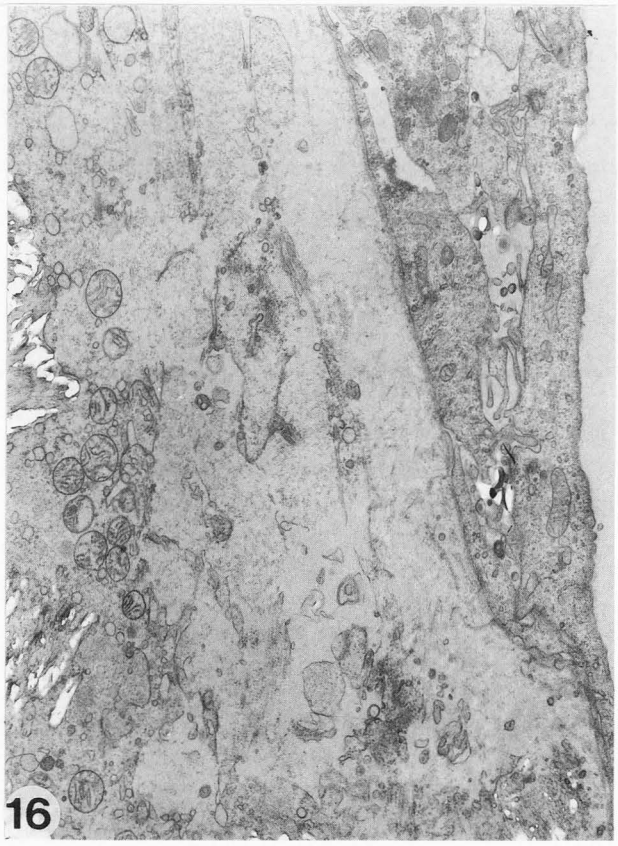
16

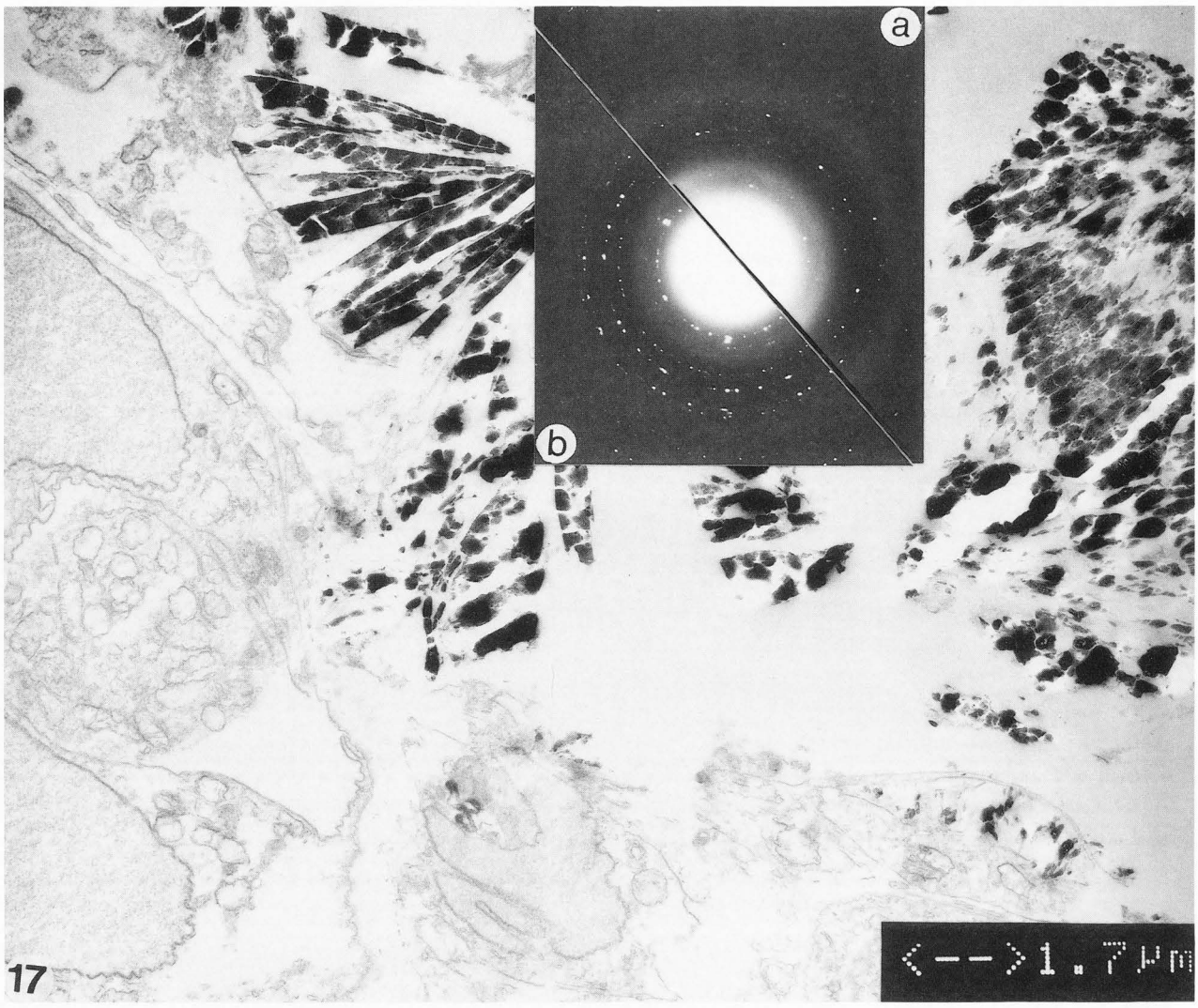

Figure 17. Transmission electron micrograph of sub-epithelial crystalline material showing the relation of crystalline material with the interstitium. In the inset, electron diffractogram of the shown crystalline material (a) compared to (b) the diffraction pattern of pure COM crystals.

---

that given before by Haggitt and Pitcock [16]. But on close inspection, these depositions are different with respect to the absence of any intertubular calcium deposits in our Von Kossa staining.

The (ultra)structural information is added to this paper to gain insight in: (1) whether this animal-model system can produce papillary lesions; (2) whether their origin as intratubular or interstitial can be established; and (3) whether there is a structural relation with the free crystals in the calycine space and/or in the fornix.

The first question can be answered positively. In the papillar areas investigated in detail after CID plus three, five or ten days recovery, sub-epithelial lesions consist of crystal masses surrounded by cells. Their interstitial presence is shown and their intratubular origin demonstrated. In addition, in the calycine space, free bare crystals are observed at or outside the papillary surface. Their origin remains to be determined. The details shown in Figures 5, 8, 14, 15 and 16, suggest the presence of a process of free-crystal enrobing outside the original papillary surface by unidentified cuboidal cells that form a pseudo-eurothelium all over the original papillary surface. The lesions do develop during the recovery phase. The time needed for "development" in rats is reduced from ten weeks [34] to $\leq$ ten days. It may occur after the episode of acute changes $\leq$ 72 hours as described by Khan *et al.* [22]. The next paper reports papillary tip changes observed by SEM [10].

The design of our experiments was to investigate the fate of retained crystals. However, in retrospect, our study differs only slightly from previous experiments reported by Vermeulen *et al.* [34, 35]. Their experiments, using a four day regime with an oral triggering dose and a maintenance dose one quarter of the triggering dose of oxamide (a diamide of oxalic acid), were designed for generation of papillary-plaque lesions. In additional experiments with an high EG regime to provoke oxaluria and a lower EG dose as maintenance, similar observations were mentioned [34]. More or less unexpected, papillary lesions described as Randall's plaques of COM crystals were observed in (two out of eighteen) animals after ten weeks on a normal drinking regime in: "short segments of adjacent collecting ducts coursing just beneath the urothelium of the papilla, ... some distance above the osteal ducts and clearly intraluminal, though formed ten weeks previously" [cited from: 34]. Our observations confirm the papillary localization but are in conflict with that description in the sense that we prefer to interpret the crystal masses (Figs. 2, 4, 14, 15 and 16) as interstitial crystals after exotubulosis, some with a sub-epithelial localization, and not as intraluminal crystals.

Moreover, our observations on the rat's papilla are different from those made earlier by Randall on human ones [30], describing milky spots as sub-epithelial peritubular calcification, identified by Von Kossa's stain and theorized to start as local necrosis. Both the former and the latter are not confirmed by our observations. We observed free crystal agglomerates plus crystals covered by unidentified cells bulging in the calycine space (Figs. 5, 8, 14, 15 and 16), and large sub-epithelial crystal masses, but there was no structural relation whatsoever with sub-epithelial calcifications. The lesions described here differ from the ones described by Randall as mini-stones on an initial or pre-calculus lesion. This relation will be further investigated by combined SEM/LM observations of papilla from similar experiments [10].

We agree with Vermeulen's idea about a "triggering dose". There must be an initial intra-nephronic episode in which the inorganic concentrations are raised and surpass the level of the formation product and crystals are created of sizes ranging from nanometers to micrometers. It has been assumed, that such crystals can pass freely through the nephron as long as their overall size is smaller than the diameter of the tubules [12, 18]. Recently, previous calculations on this dynamic aspect, have been adopted [25]. The basic concept of crystal transport through the nephron, mainly based upon the frequency of occurrence of crystals in the various (how well-defined?) nephron segments, is in spatial resolution terms only coarsely supported by experiments with ^{14}C-oxalate salts [1] in "acute" experiments. Although the existence of intraluminal crystal transport is not denied, the results of our previous [9] and present experiments may attribute components for improvements. In our CID-model, previous observations indicate that additional processes interfere with the initially formed inorganic crystal's viz.: (a) opsonization and/or (b) aggregation and/or (c) adherence/non-adherence to structural components in the cellular apex [9]. Several endogenous and exogenous opsonization/aggregation/adhesion(?) regulating (glyco)proteins are known, isolated and chemically identified [13, 17, 26-27, 31-33]. The main question is now to confirm this interference process along the nephron and to establish when, where and how it takes place. Knowledge about the subsequent steps in this nephrolithic process not only might be beneficial for the patients, it might also be the "last chance" for exogenous drugs to interfere with intratubular crystals. For the papillary area, new pathognostic events might have to be considered, e.g., about the fate of the interstitial crystal masses and the role of the Randall's plaques therein.

With respect to the idea of Vermeulen *et al.* [34, 35] about a "maintenance dose", we accept that in the experimental set-up this is important and allows one to study the conversion of retained crystals into stones. The presence of a "maintenance dose" might be of importance in stone formers in which chronically raised metabolites levels are present or when there are episodes of recurrent alternations in the metabolite concentrations concerned. It might be speculated that, in our chronic experimental CID rat model, tissue/blood oxalate and calcium concentrations might also alternate in a certain rhythm, related to the drinking habits of the rats. Hence, the initial inorganic crystal size and the subsequent crystal appearance may represent these changes, which remains to be investigated. This rat model shows the presence and the structural details of papillary lesions. However, most lesions differ from those described before both in rat and in human.

Acknowledgements

The financial support of the Dutch Kidney Foundation (ER Boevé, R de Water and PPMC van Miert, grant 92.1235) and the SUWO (Stichting urologisch wetenschappelijk onderzoek) is acknowledged.

References

1. Blumenfrucht MJ, Cheeks C, Weden RP (1986) Multiorgan crystal deposition following intravenous oxalate infusion in rat. J Urol **135**: 1274-1279.

2. Boevé ER, Ketelaars GAM, Vermey M, Cao LC, Schröder FH, de Bruijn WC (1993) An ultrastructural study of experimentally induced microliths in rat proximal and distal tubules I. J Urol **149**: 893-899.

3. Cao LC, Boevé ER, Schröder FH (1991) The mechanisms of action of glycosaminoglycans (GAG's) in calcium oxalate stone prevention: A review. J Lithotripsy Stone Dis **3**: 324-333.

4. Cao LC, Boevé ER, de Bruijn WC, Schröder FH (1993) A review of new concepts in renal stone research. Scanning Microsc **7**: 1049-1065.

5. Cifuentes-Delatte L, Minon-Cifuentes J, Medina JA (1987) New studies on papillary calculi. J Urol **137**: 1024-1029.

6. Daudon M, Jungers P (1991) Methodes d'analyse des calculs et cristaux urinaires (Analytical methods for urinary stones and crystals). Rev-Prat **41**: 2017-2022.

7. De Bruijn WC (1973) Glycogen, its chemistry and morphologic appearance in the electron microscope I. A modified OsO_4 fixative which selectively contrasts glycogen. J Ultrastruct Res **42**: 29-44.

8. De Bruijn WC, Ketelaars GAM, Boevé ER, Sorber CWJ, Cao LC, Schröder FH (1993) Electron energy-loss spectroscopical and image analysis of experimentally induced microliths II. J Urol **149**: 900-905.

9. De Bruijn WC, Boevé ER, van Run PRWA, van Miert PPMC, Romijn JC, Verkoelen CF, Cao LC, Schröder FH (1994) Etiology of experimental calcium oxalate monohydrate nephrolithiasis in rats. Scanning Microsc **8**: 541-550.

10. De Bruijn WC, Boevé ER, van Run PRWA, van Miert PPMC, Romijn JC, Verkoelen CF, Cao LC, van't Noordende JM, Schröder FH (1995) Etiology of calcium oxalate nephrolithiasis in rats. II. The role of the papilla in stone formation? Scanning Microsc **9**: (this issue).

11. Dijkstra M, Hackett RL (1979) Ultrastructural events in early calcium oxalate crystal formation in rats. Kidney Intern **15**: 640-650.

12. Finlayson B, Reid F (1978) The expectation of free and fixed particles in urinary stone disease. Invest Urol **15**: 442-448.

13. Gokhale JH, Glenton PA, Khan SR (1994) Analysis of Tamm-Horsfall protein in a rat model of nephrolithiasis. Proc. 5th Europ. Urolithiasis Symp. Rao PN, Kavanagh JP, Tiselius H-G (eds.). Publ. by Rao and Kavanagh, Lithotriptor Unit, Univ. Hospital of So. Manchester, Manchester, M20 8LR, UK. pp. 91-92.

14. Grases F, Costa-Bauzá A, Conte A (1993). Studies on structure of calcium oxalate monohydrate renal papillary calculi. Mechanism of formation. Scanning Microsc **7**: 1067-1074.

15. Hackett RL, Shevock PV, Khan SR (1990) Cell injury associated calcium oxalate crystalluria. J Urol **144**: 1535-1545.

16. Haggitt RC, Pitcock JA (1971) Renal medullar calcifications: A light and electron microscopic study. J Urol **106**: 342-347.

17. Hess B (1994) Tamm-Horsfall Mucoprotein. Proc. 5th Europ. Urolithiasis Symp. Manchester. *op. cit.* 22-23.

18. Jordan WR, Finlayson B, Luxenberg M (1978) Kinetics of early time calcium oxalate nephrolithiasis. Invest Urol **15**: 465-468.

19. Karlowicz MG, Katz ME, Adelman RD, Solhaug MJ (1993) Nephrocalcinosis in very low birth weight neonates: Family history of kidney stones and ethnicity as independent risk factors. J Pediatrics **122**: 635-638.

20. Khan SR (1991) Pathogenesis of oxalate urolithiasis: Lessons from experimental studies with rats. Am J Kidn Dis **17**: 398-401.

21. Khan SR, Finlayson B, Hackett RL (1979) Histology study of the early events in oxalate induced intranephronic calculosis. J Urol **17**: 199-202.

22. Khan SR, Finlayson B, Hackett RL (1982) Experimental calcium oxalate nephrolithiasis in the rat. The role of the renal papilla. Am J Pathol **107**: 59-69.

23. Khan SR, Shevock PN, Hackett RL, (1989) Urinary enzymes and calcium oxalate urolithiasis. J Urol **142**: 840-849.

24. Khan SR, Shevock PN, Hackett RL (1992) Acute hyperoxaluria, renal injury and calcium oxalate urolithiasis. J Urol **147**: 226-230.

25. Kok DJ, Khan SR (1994) Calcium oxalate nephrolithiasis, a free or fixed particle disease. Kidney Intern **46**: 847-854.

26. Nakagawa Y, Abram V, Kézdy F, Kaiser ET, Coe FL (1983) Purification and characterization of the principal inhibitor of calcium oxalate monohydrate crystal growth in human urine. J Biol Chem **258**: 12594-12600.

27. Netzer M (1994) Nephrocalcin. Proc. 5th Europ. Urolithiasis Symp. Manchester. *op. cit.* 22-23.

28. Mijan JL, Aneiros J, O'Valle F, Zuloaga A, Martinez JL, Camara M (1988) Experimental oxalosis in rats: An electron microscopic study. Urol Int **43**: 19-23.

29. Öhman S, Larsson L (1992) Evidence for Randall's plaques to be the origin of primary renal stones. Med Hypoth **39**: 360-363.

30. Randall A. (1940) The etiology of primary renal calculus. Int Abst Surg **71**: 209-240.

31. Rose GA, Sulaiman S (1982) Tamm-Horsfall mucoproteins promote calcium oxalate crystal formation in urine: Quantitative studies. J Urol **127**: 177-179.

32. Sirivongs D, Nakagawa Y, Vishny WK, Favus MJ, Coe FL (1989) Evidence that mouse renal proximal tubule cells produce nephrocalcine. Am J Physiol **26**: F390-F398.

33. Stapleton AMF, Ryall RL (1994) Novel developments of a specific antibody to prothrombin fragment 1: crystal matrix protein exposed as an F1 alias. Proc. 5th Europ. Urolithiasis Symp. Manchester. *op. cit.* 92-93.

34. Vermeulen CW, Lyon ES (1968) Mechanisms of genesis and growth of calculi. Amer J Med **45**: 684-689.

35. Vermeulen CW, Lyon ES Ellis JE, Borden TA (1967) The renal papilla and calculogenesis. J Urol **97**: 573-579.

36. Wright RJ, Hodgkinson A (1972) Oxalic acid, calcium and phosphorus in the renal papilla of normal and stone forming rats. Invest Urol **9**: 369-375.

Note: Please see part 2 of this paper (which follows) for **Discussion with Reviewers**.